Supporting Information

Catalysis of GTP hydrolysis by small GTPases at atomic detail by integration of X-ray crystallography, experimental and theoretical IR spectroscopy

Till Rudack[†,‡], Sarah Jenrich[†,‡], Sven Brucker[†], Ingrid R. Vetter[#], Klaus Gerwert[†,⊥,*], and Carsten Kötting[†,*]

[†]Biophysics, University of Bochum, Universitaetstrasse 150, 44780 Bochum, Germany

[#]Max-Planck-Institut für Molekulare Physiologie, Otto-Hahn-Strasse 11, 44227 Dortmund, Germany

[⊥]Chinese Academy of Sciences-Max Planck Partner Institute and Key Laboratory for Computational Biology, Shanghai Institutes for Biological Sciences, 320 Yue Yang Road, Shanghai, 200031, China

Supplemental Table S1. Simulation systems with the Mg^{2+} coordination, numbers of amino acids, solute atoms, water molecules, and counter-ions. The MD simulations of Ras base on the X-ray structure 1QRA. Note that during the equilibration of the structure the Tyr32 flipped into the GTP binding niche and forms a hydrogen bond to an oxygen atom of the γ-phosphate. This is the canonical structure found in most X-ray structures. The MD simulations of Ran base on the X-ray structure 1RRP.

Simulation System	Mg^{2+}	Amino acids	Water Molecules	Na^+	Cl^-	Solute Atoms
RasWT·GTP·Mg^{2+}	βγ	1-166	21884	61	61	2674
RasWT·GTP·Mg^{2+}	αβγ	1-166	21884	61	61	2674
RanWT·GTP·Mg^{2+}·RanBP1	βγ	8-211/ 17-150	43242	122	122	5542
RanWT·GTP·Mg^{2+}·RanBP1	αβγ	8-211/ 17-150	43242	122	122	5542
RasA18T·GTP·Mg^{2+}	βγ	1-166	21884	61	61	2678
RanT25A·GTP·Mg^{2+}·RanBP1	βγ	8-211/ 17-150	43019	121	121	5538
RanT25A·GTP·Mg^{2+}·RanBP1	αβγ	8-211/ 17-150	43019	121	121	5538
RasY32A·GTP·Mg^{2+}	βγ	1-166	21882	61	61	2663
RanY39A·GTP·Mg^{2+}·RanBP1	βγ	4-215/ 22-151	49130	138	138	5562

Supplemental Table S2: B-factors of the Gln69/Gln61 side chains of the X-ray structures of RanWT (1RRP) with RanT39A and the simulated B-Factors calculated from the 50 ns trajectories of the MD simulations of RasWT, RasY32A, RanWT and RanT39A. The trajectories are fitted to the averaged structure and then the standard deviation σ of the atomic positions in the trajectory is calculated. The B-factor is $8\pi\sigma^2$. The values are the average of the B-factors of all side chains atoms of Gln69/Gln61. The B-factors are given in the unit $Å^2$.

	RasWT	RasY32A	Δ	RanWT	RanT39A	Δ
X-ray	--	--		71	87	16
MD	19	19	0	12	26	14

Supplemental Section S1. Details of the new RanY39A·RanBD1 structure

We crystallized the RanY39A·GppNHp·RanBD1 complex (RanY39A·RanBD1 in the following) and solve the structure with 3.2 A resolution. Here, several alterations compared to the Ran wildtype complex with RanBD1 (1RRP) were observed. While the two RanΔ191·GDP·BeF·RanBD1 complexes (Ran·RanBD1 in the following) in the asymmetric unit are very similar to each other (and thus were compatible with tight NCS constraints, see methods), 1RRP and RanY39A· RanBD1 show relative rotations of 4° and 3.3°, respectively, between the Ran and RanBD1 domains of the two complexes in the asymmetric unit. RanY39A·RanBD1 compared to 1RRP shows rotations between 3.4° and 8.9°, Ran· RanBD1 compared to 1RRP even 7.8°-11.7°. Ran·RanBD1 and RanY39A·RanBD1 are more similar with values between 2.9° and 5.7°. This means that no two rotations are similar except for the two Ran· RanBD1 complexes in the asymmetric unit, indicating that the interface is relatively variable and that interactions outside of the interface (e.g. the N-terminus of the RanBD1 domain) contribute to the interaction. In addition, RanY39A· RanBD1 exhibits a slightly different position of the Ran C-terminal helix, but with a conserved position of the start of the ^{211}DEDDDL^{216} motif (in both 1RRP and RanY39A·RanBD1 the last amino acid with a well-defined electron density is Asp211). Interestingly, a disulfide bridge is formed between the cysteines 142 of two symmetry related neighboring RanBD1 molecules in both complexes of the asymmetric unit, which might contribute to the observed differences.

Another difference compared to 1RRP and Ran·RanBD1 is a shift of the N-terminus of RanBD1. In one complex in the asymmetric unit, the defined electron density ends with residue 22 with weak density for the following residues 21-15 that are in the “canonical” position. In the other complex density stops with residue 19, and the “canonical” position is blocked by a symmetry related molecule so that residues 19-24 follow a different path compared to 1RRP and Ran·RanBD1.

Six putative sulfate ions, i.e. blobs of electron density that were too strong for water, are observed in the RanY39A·RanBD1 structure as it was crystallized in 1.8 M ammonium sulfate. One binding site is formed by rearrangement of Arg140 of RanY39A (that contributes to the “basic patch” that fixes the C-terminal 211DEDDDL216 motif of Ran in the Ran·GDP form). The Arg140 side chain has moved together with the short helix that contains R140 compared to 1RRP and Ran·RanBD1. Otherwise it would clash with a neighboring molecule in the RanY39A·RanBD1 structure. The resulting conformational change pushes loop 141-144 in direction of the canonical binding site of the RanBD1 N-terminus so that it is displaced relative to 1RRP as described above. Interestingly, a very similar conformation of the region 130-144 was observed in the Ran-Importin beta complex 3EA5 (1). In general, this stretch is relatively variable when comparing all other available Ran structures. In chain C of the RanY39A·RanBD1 structure, residues 140-143 are disordered so that the N-terminus of RanBD1 (chain D) can assume its canonical place. The rearranged arginine side chain of Ran in the first RanY39A·RanBD1 complex (chains A and B) forms a binding site for a putative sulfate ion close to His105 and Pro102 of the same Ran chain. Another sulfate ion is observed close to Arg108 of RanBD1 that corresponds to the basic patch of RanBD1 that also interacts with the DEDDDL motif of the Ran C-terminal helix, confirming the preference of this region for negative charges.

References:

1. Forwood, J. K., Lonhienne, T. G., Marfori, M., Robin, G., Meng, W., Guncar, G., Liu, S. M., Stewart, M., Carroll, B. J., and Kobe, B. (2008) Kap95p binding induces the switch loops of RanGDP to adopt the GTP-bound conformation: implications for nuclear import complex assembly dynamics. *J. Mol. Biol.* **383**, 772–782

Supplemental Table S3: X-ray data collection and refinement statistics

	Ran191-RanBD1	**RanY39A-RanBD1**	**Ran GDP**	**Ran GDP**	**RanY39A GDP**	**RanY39A GDP**
pdb code	5CLL	5CLQ	5CIQ	5CIT	5CJ2	5CIW
Space group complex/AU	P21 2	C2221 2	P41 2	P21 2	P1 8	P21 8
Detector	MarCCD	Pilatus 6M	MarCCD	MarCCD	MarCCD	MarCCD
a,b,c (Å)	50.6 55.8 122.9	102.5 170.9 135.7	102.7 102.7 41.9	58.0 59.2 64.8	59.2 80.7 91.7	57.9 59.3 64.8
α, β, γ (°)	90.00 90.01 90.0	90.0 90.0 90.0	90 90 90	90 97.0 90	97.7 90.0 90.0	90 96.6 90
Resolution (Å)	2.45 (2.51-2.45)*	3.2 (3.28-3.2)*	1.65 (1.69-1.65)*	1.75 (1.8-1.75)*	1.75 (1.8-1.75)*	1.75 (1.8-1.75)*
R_{sym}	8.2(29.1)*	9.4(87.1)*	5.0(58.5)*	3.7(64.1)*	3.7(36.8)*	3.4(27.5)*
$I/\sigma I$	10.17(2.97)*	16.99(2.97)*	18.1(2.1)*	17.9(2.1)*	14.4(2.5)*	23.4(4.9)*
Completeness (%)	95.9(75.3)*	99.4(99.9)*	98.2(85.7)*	96.2(95.8)*	92.2(81.5)*	94.7(80.3)*
Redundancy	3.4(1.8)*	6.6(6.9)*	4.5(2.5)*	3.3(3.4)*	2.0(1.7)*	3.6(3.0)*
Refinement:						
Resolution (Å)	50.6-2.45	19.98-3.2	38.78-1.65	19.84-1.75	47.59-1.75	19.89-1.75
No. reflections	23356	19894	49469	40327	148638	39746
*R*work / *R*free	23.5/27.2	22.4/25.4	19.8/25.1	21.8/26.5	19.8/24.1	20.1/25.0
No. atoms:						
Protein/ Ligands	5181/66	5416/96	3221/58	3186/58	12725/246	3196/58
Water	33	12	157	86	425	113
aver. B (Å2)	22.3	89.3	25.5	37.0	28.6	29.8
R.m.s. deviations:						
Bond lengths (Å)	0.007	0.010	0.012	0.022	0.020	0.020
Bond angles (°)	1.282	2.005	2.329	2.280	2.206	2.180

* Values in parentheses are for highest resolution shell

Supplemental Section S2. Used X-Ray structures in Figure 1 c
1RRP, 1K5D, 1QBK, 1WA5, 2BKU, 2X19, 3A6P, 3ICQ, 3M1I, 3NC0, 3NC1, 3W3Z, 3ZJY, 4HAT, 4HAU, 4HAV, 4HAW, 4HAX, 4HAY,4HAZ, 4HB0, 4HB2, 4HB3, 4HB4

Supplemental Section S3. Used X-Ray structures in Figure 4
a) Complexed Ras structures:
2uzi, 2vh5, 3ddc, 2c5l, 1k8r, 1lfd, 1he8, 4g0n, 4g3x, 1nvv, 1nvw, 1nvu, 1nvx, 4k81
b) Complexed Ran structures:
1rrp, 1ibr, 1qbk, 1wa5, 2bku, 2x19, 3a6p, 3gjx, 3icq, 3m1i, 3nby, 3nbz, 3nc0, 3nc1, 3w3z, 3zjy, 4c0q, 4gmx, 4gpt, 4hat, 4hau, 4hav, 4haw, 4hax, 4hay, 4haz, 4hb0, 4hb2, 4hb3, 4hb4, 1k5d,
c) Complexed Rab structures:
4d0l, 3tkl, 1zbd, 3bc1, 2zet, 1tu3, 3mjh, 3bbp, 3cwz, 1yhn, 1z0k, 2d7c, 2hv8, 2gzd, 2gzh, 4c4p, 3tso, 3qbt, 3tnf, 1z0j, 4lhz
d) Uncomplexed H-Ras structures:
5p21, 1p2s, 1p2t, 1p2u, 1p2v, 1ctq, 3tgp, 3k9n, 3k9l, 2rge, 3k8y, 3lbh, 3lbi, 3lbn, 3oiu, 3oiv, 3oiw, 3l8y, 3l8z, 3rry, 3rrz, 3rs0, 3rs2, 3rs3, 3rs4, 3rs5, 3rs7, 3rsl, 3rso, 3v4f, 4dlr, 4dls, 4dlt, 4dlu, 4dlv, 4dlw, 4dlx, 4dly, 4dlz, 4efl, 4efm, 4efn, 6q21, 121p, 1qra, 421p, 1jah, 221p, 521p, 621p, 721p, 821p, 1jai, 2rgg, 1lf0, 1zw6, 2rgb, 2rgc, 2rga, 2rgd, 3i3s, 4l9w, 3kkm, 3kkn, 1xcm, 1iaq, 1agp
e) Uncomplexed Rab structures:
3nkv, 3rab, 2bme, 1yu9, 1n6h, 1n6o, 1n6p, 1n6l, 1n6r, 1r2q, 1huq, 1z07, 1yzq, 2y8e, 2gil, 2ffq, 1t91, 1vg8, 3law, 4lhw, 1yzl, 2ocb, 1yzk, 1oiw, 2f9m, 1x3s, 1z08, 1yzt, 1yzu, 1yvd, 2g6b, 3e5h, 2ew1, 2fg5, 1z06, 1yzn, 1ky2, 1ek0, 1g17

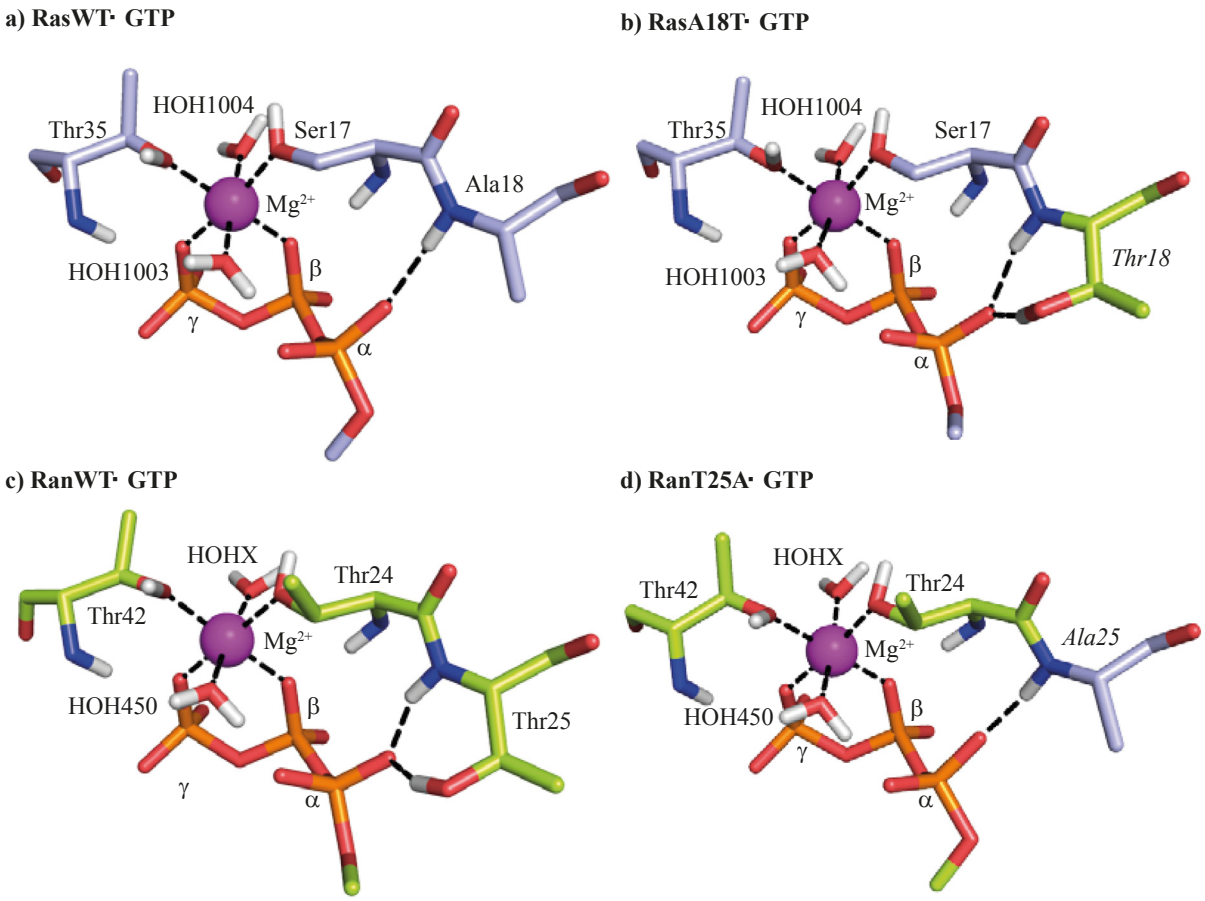

Supplemental Figure S1: Comparison of the averaged structures of the equilibrated last 25 ns of 50 ns molecular dynamics simulations of solvated RasWT·GTP·Mg^{2+}·RanBD1 (light blue carbon atoms) (a) and RasA18T·GTP·Mg^{2+} (b) as well as RanWT·GTP·Mg^{2+}·RanBD1 (light green carbon atoms) (c) and RanT25A·GTP·Mg^{2+}·RanBD1 (d). In (c) and (d) the second water molecule HOHX does not exist in the X-ray structure of RanWT·RanBD1 (1RRP) and has been added referring to the Ras structure of the βγ-form. In all four 50 ns simulation trajectories of Ran and Ras the Mg^{2+} is βγ-coordinated in the starting structure and remained stably bidentately coordinated by the triphosphate. Oxygen atoms are red, nitrogen atoms are blue, phosphate atoms are orange, hydrogen atoms are light grey, and the magnesium ion is purple.

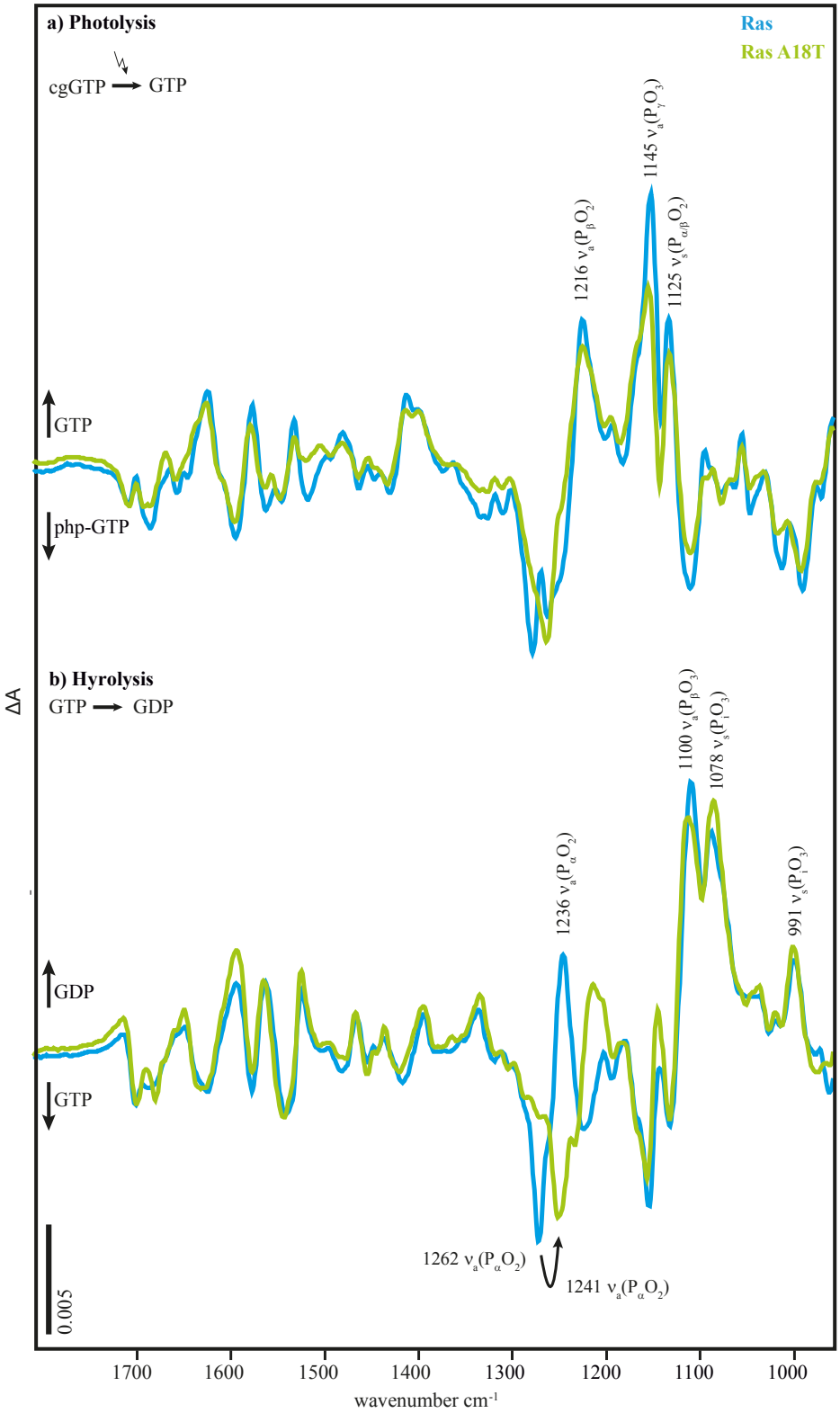

Supplemental Figure S2: The phosphate and amide region of the FTIR difference spectra of the photolysis reaction a_{ph} (a) and hydrolysis reaction a_{hyd} (b) in RasWT (blue) and RasA18T (green). The mutant is scaled by factor 3.

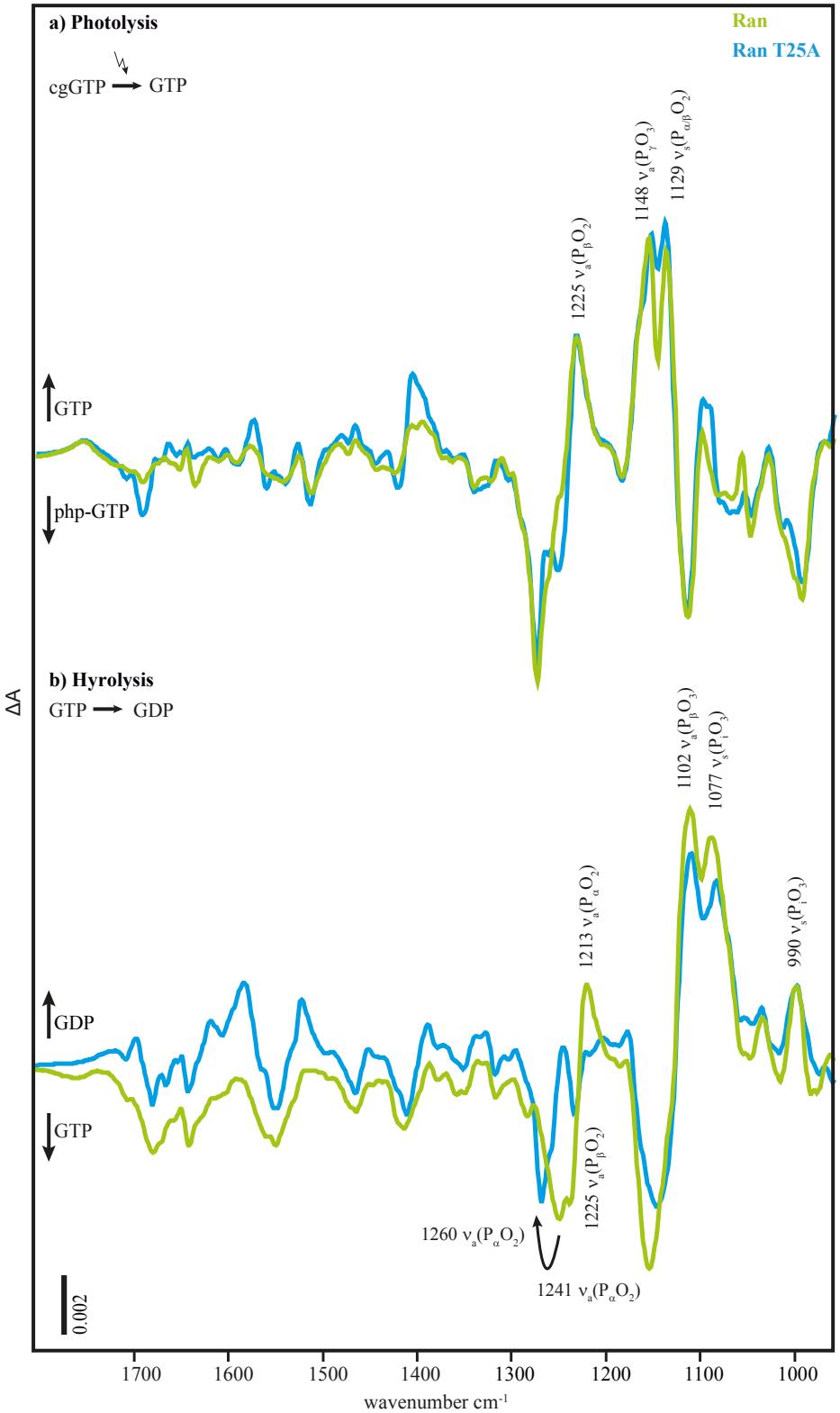

Supplemental Figure S3: The phosphate and amide region of the FTIR difference spectra of the photolysis reaction a_{ph} (a) and hydrolysis reaction a_{hyd} (b) in RanWT·RanBD1 (green) and RanT25A·RanBD1 (blue). The mutant is scaled by factor 2.

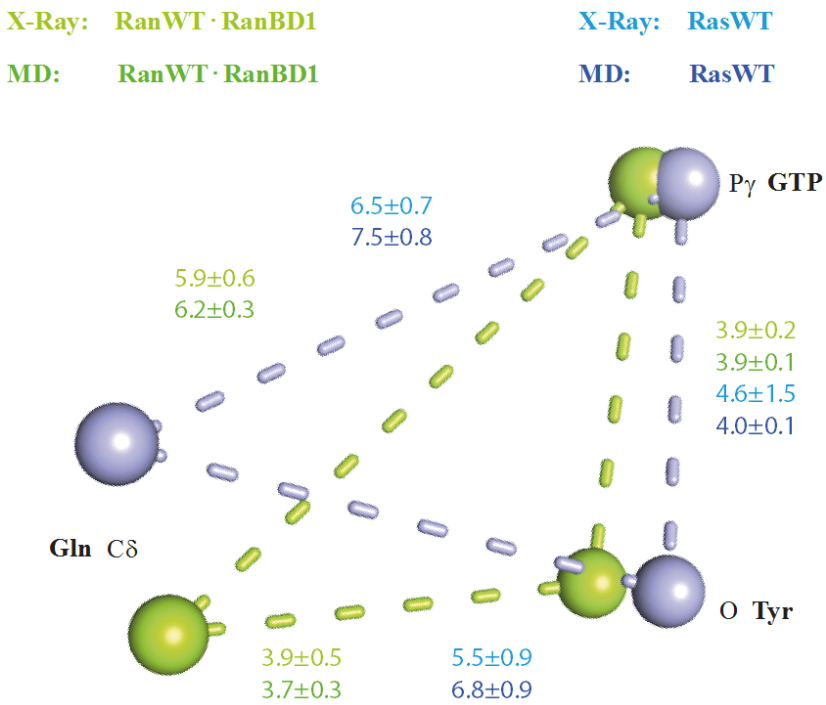

Supplemental Figure S4: Comparison of the distances of the key residues in Ras and Ran. Given are the distances between the oxygen atom of the Tyr side chain (32 in Ras and 39 in Ran), the Cδ atom of the Gln (61 in Ras and 69 in Ran) and the phosphor atom of the γ-phosphate. The values are averaged over the published complexed X-ray structures of Ras and Ran compared to the averaged values of the MD simulation trajectories. All values are given in Å. The used X-Ray structures for the values in this figure and in Figure 7 c are:
Complexed H-Ras structures: 2uzi, 2vh5, 3ddc, 2c5l, 1k8r, 1lfd, 1he8, 4g0n, 1nvv, 1nvw, 1nvu, 1nvx, 4k81
Complexed Ran structures: 1rrp, 1ibr, 1qbk, 1wa5, 2bku, 3a6p, 3w3z, 4gmx, 4gpt, 4hat, 4hau, 4hav, 4haw, 4hax, 4hay, 4haz, 4hb0, 4hb2, 4hb3, 4hb4, 1k5d